THE JOURNAL OF PHYSICAL CHEMISTRY B

Article

pubs.acs.org/JPCB

Spectral Resolution of the Primary Electron Acceptor A_0 in Photosystem I

Adrien Chauvet,[†] Naranbaatar Dashdorj,[‡] John H. Golbeck,[§] T. Wade Johnson,[¶] and Sergei Savikhin*[,†]

[†]Department of Physics, Purdue University, 525 Northwestern Ave, West Lafayette, Indiana 47907, United States

[‡]Argonne National Laboratory, 9700 S. Cass Ave, 433/D006, Argonne, Illinois 60439, United States

[§]Department of Biochemistry and Molecular Biology, and Department of Chemistry, The Pennsylvania State University, 310 South Frear Laboratory, University Park, Pennsylvania 16802, United States

[¶]Department of Chemistry, Susquehanna University, 514 University Ave, Selinsgrove, Pennsylvania 17870, United States

ABSTRACT: The reduced state of the primary electron acceptor of Photosystem I, A_0, was resolved spectroscopically in its lowest energy Q_y region for the first time without the addition of chemical reducing agents and without extensive data manipulation. To carry this out, we used the *menB* mutant of *Synechocystis* sp. PCC 6803 in which phylloquinone is replaced by plastoquinone-9 in the A_1 sites of Photosystem I. The presence of plastoquinone-9 slows electron transfer from A_0 to A_1, leading to a long-lived A_0^- state. This allows its spectral signature to be readily detected in a time-resolved optical pump−probe experiment. The maximum bleaching ($A_0^- - A_0$) was found to occur at 684 nm with a corresponding extinction coefficient of 43 mM^{-1} cm^{-1}. The data show evidence for an electrochromic shift of an accessory chlorophyll pigment, suggesting that the latter Q_y absorption band is centered around 682 nm.

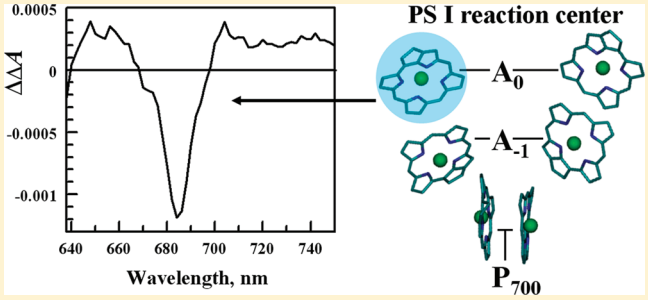

INTRODUCTION

The Photosystem I (PS I) pigment−protein complex is a critical component of the oxygenic photosynthetic apparatus, and is common to plants, green algae, and cyanobacteria. PS I utilizes light to generate reduced ferrodoxin and NADPH, which in turn drives a wide variety of biochemical processes.[1,2] Its X-ray crystal structure has been refined to 2.5 Å, revealing ∼100 chlorophyll (Chl) *a* pigments embedded primarily in two core PS I proteins, PsaA and PsaB.[3] Most of these Chls serve as light-harvesting antenna and rapidly transfer light excitation energy to the reaction center (RC) core. This results in initial charge separation and subsequent transfer of the electron toward the stromal side of the membrane where it reduces the soluble protein, ferredoxin. The heart of the RC consists of six Chl molecules, two phylloquinones (PhQ), and three [4Fe-4S] clusters (F_x, F_A, F_B). The six Chls and the PhQs are arranged in two branches, A and B, as pairs of molecules related by pseudo-C_2 rotational symmetry, shown in Figure 1. The strongly coupled chlorophylls eC-A1 and eC-B1 serve as electron donor and are usually referred to as the special pair P_{700}; the eC-A2 and eC-B2 pigments are referred to as accessory Chls (A_{-1}) and facilitate the initial charge separation process, and the eC-A3 and eC-B3 serve as primary electron acceptors and are denoted as A_0. The two secondary electron acceptors, phylloquinones Q_k-A and Q_k-B, are denoted A_1. The trapping of the electronic excitation created by the absorption of a photon by the PS I antenna occurs in the RC and requires ∼10−70 ps, depending on the species,[4] resulting in the formation of the initial charge separated state $P_{700}^+A_0^-$. Subsequent electron transfer leads to the long-lived charge-separated state $P_{700}^+F_B^-$. The sequence of events can be written as

$$[\mathrm{Ant}]^* \leftrightarrow [\mathrm{RC}]^* \rightarrow P_{700}^+A_0^- \rightarrow P_{700}^+A_1^- \rightarrow P_{700}^+F_X^- \rightarrow P_{700}^+F_A^- \rightarrow P_{700}^+F_B^-$$

where [Ant]* represents PS I where one of the antenna pigments is in excited state and [RC]* corresponds to the excitation residing on the reaction center.

According to the most recent experimental data, the primary electron-transfer step may involve charge separation between the nearby accessory Chls and A_0, followed by electron transfer from P_{700} to the oxidized accessory Chl and the formation of $P_{700}^+A_0^-$.[5,6] Note that electron transfer in PS I occurs primarily along A-branch.[7−10]

The energy-transfer and initial electron-transport steps in PS I can only be revealed by ultrafast laser spectroscopy. However, both the light-harvesting antenna pigments as well as the primary electron-transfer cofactors are Chl *a* molecules that absorb light around 680 nm. This spectral congestion precludes resolution of the optical spectra of the individual pigments. It also complicates clear separation of the kinetics into different

Received: November 22, 2011
Revised: February 14, 2012
Published: February 14, 2012

   dx.doi.org/10.1021/jp211246a | *J. Phys. Chem. B* 2012, 116, 3380−3386

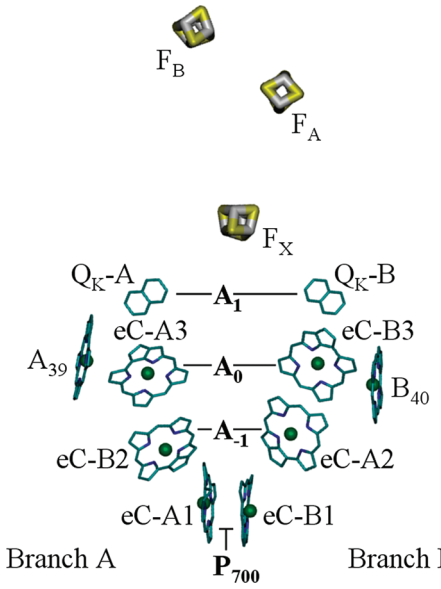

Figure 1. Crystal structure of the PS I RC cofactors involved in electron transfer and the two closest to RC (connecting) antenna pigments A_{39} and A_{40}.[3] Side chains are omitted for chlorophylls and phylloquinones for clarity.

processes as well as any detailed modeling of the energy conversion processes. Only the optical properties of the P_{700} special pair have been clearly resolved via $(P_{700}^{+} - P_{700})$ difference spectra, and this is only because long-lived P_{700}^{+} can be easily formed using light or chemical oxidants. Subunit deficient mutations have provided additional information on the optical properties of few groups of the peripheral antenna Chl *a* pigments.[11] Several attempts have been made to characterize spectroscopically the primary acceptor, A_0, that is a key player in the primary charge separation step. However, different methods used by various groups have placed the $(A_0^{-} - A_0)$ absorption difference band maximum anywhere between 685 and 695 nm, a spread of wavelengths that is comparable to the absorption bandwidth of a single chlorophyll molecule. The primary reason for this uncertainty is that the A_0^{-} state in PS I is short-lived compared to the excitation trapping time and never accumulates in the large quantities required for its clear optical detection.

Several groups have used dithionite treatment at pH of 9.0–11.5 to prereduce the secondary electron acceptor, A_1, thereby blocking electron transfer from A_0^{-} and enabling the measurement of the $(P_{700}^{+}A_0^{-} - P_{700}A_0)$ difference spectrum. In a separate experiment, the sample is treated with ferricyanide to oxidize P_{700} revealing the $(P_{700}^{+} - P_{700})$ difference spectrum. By comparing the two difference spectra, the $(A_0^{-} - A_0)$ maximum was estimated to be at either 693,[12,13] 690,[14] or 686 nm.[15] The strong chemical reductant used in these studies may influence pigment–protein interactions in PS I, which could explain the wide spread of the $(A_0^{-} - A_0)$ maxima. Moreover, the spectra of $(P_{700}^{+} - P_{700})$ and $(P_{700}^{+}A_0^{-} - P_{700}A_0)$ are often obtained under different conditions, which is an additional factor leading to uncertainty in the $(A_0^{-} - A_0)$ difference spectrum. Kim et al.[16] used PS I complexes depleted of PhQ, which corresponds to the physical removal of the secondary electron acceptors A_1, and observed an $(A_0^{-} - A_0)$ difference maximum at 686 nm. However, the solvent-based PhQ depletion process additionally removes all carotenoids and the majority of the Chl *a* pigments from PS I.[17] Reducing the antenna size of the PS I complexes by solvent treatment shortens the excitation trapping time and minimizes the spectral congestion effects that allow resolution of the A_0 spectrum. Shuvalov et al.[18] reduced the total number of pigments in PS I monomer to 26 and assigned the band at 695 nm to the $(A_0^{-} - A_0)$ spectrum. Kumazaki et al.[19] prepared PS I complexes with 16 and 30 Chl *a* pigments and reported the $(A_0^{-} - A_0)$ band at 685 nm. Wasielewski et al.[20] studied PS I particles containing 30–40 Chl *a* and found that the $(A_0^{-} - A_0)$ bleaching peaked at 690 nm. While reducing the number of pigments in PS I significantly simplifies the interpretation of experimental data, this procedure also affects the integrity of PS I, as the carotenoid and Chl pigments are a structural part of this protein complex.

Other groups have attempted to resolve the A_0^{-} spectrum without alteration of the pigment–protein complex. Hasting et al.[15] used very high energy laser pulses that created 6–8 excitations per PS I to shorten the antenna lifetime from ~25 to ~4 ps due to excitation annihilation. This approach enabled them to resolve a 21 ps decay component in a decay-associated spectrum (DAS) that showed a maximum at 686 nm and it was ascribed to A_0^{-} oxidation kinetics. However, this method is model-dependent and ignores the fact that excitation annihilation in antenna cannot in general be described by a single exponential (and thus may contribute to the 21 ps DAS component). White et al.[21] subtracted the $(P_{700}^{+} - P_{700})$ absorption difference spectrum measured at long times after excitation from multiple transient spectra taken at early times. The difference spectrum that exhibited the strongest signal peaked at 685 nm and was interpreted as the $(A_0^{-} - A_0)$ difference spectrum. This approach assumes that the A_0 and P_{700} spectra do not overlap, an assumption that ultimately affects the resulting spectrum. A similar method was used by Savikhin et al.[22] to resolve the $(A_0^{-} - A_0)$ difference spectrum by subtraction of a later time spectrum (200 ps) from an early time spectrum (8 ps). The results were also model-dependent as they relied on a kinetic model derived from the experimental data.

In this paper, we use the *menB* mutant of *Synechocystis* sp. PCC 6803[23] of PS I (hereafter called *menB* PSI) to obtain the $(A_0^{-} - A_0)$ difference spectrum without chemical treatment of the sample. In this mutant, the biosynthesis of PhQ is interrupted while the PS I pigment–protein complex is not affected in any other way. In the absence of PhQ, PS I remains functional, as it incorporates plastoquinone-9 (PQ-9) in A_1 sites.[24] We found that under our experimental conditions the $A_0^{-} \rightarrow A_1$ electron transfer in *menB* PS I complexes slows down considerably and the A_0^{-} state can be unambiguously resolved at times of ~100 ps when there are no residual excitations in the antenna. Our data shows that A_0 maximally absorbs at 682–684 nm, and also suggests that a nearby accessory Chl *a* pigment absorbs at about the same wavelength.

MATERIAL AND METHODS

Ultrafast Spectroscopy. The optical pump–probe spectroscopy system has been described in detail elsewhere.[25,26] Pulses from a self-mode-locked Ti:sapphire laser were amplified by a factor of $\sim 10^5$ at 1 kHz repetition rate in a regenerative amplifier. The 780 nm output was recompressed to ~90–100 fs duration using a grating pair, and converted to an infrared signal and idler pulses in a Type I BBO optical parametric amplifier.[27] The signal output pulses were frequency-doubled into tunable visible light pulses (600–730 nm), which served as

dx.doi.org/10.1021/jp211246a | J. Phys. Chem. B 2012, 116, 3380–3386

sample excitation pulses. The sample absorption was probed with broadband continuum light pulses generated in a sapphire plate; cross correlations between the pump and probe pulses were typically 100−200 fs fwhm. Continuum pulses were split into signal and reference beams, dispersed in an Oriel MS257 imaging monochromator operated at ∼2 nm band-pass, and directed onto separate Hamamatsu S3071 Si pin photodiodes. The pump intensity was monitored and digitized, along with the transmitted signal and reference beams. This permitted digital noise filtering, whereby noise spikes (e.g., arising from sample particulates) were eliminated; this improved the signal/noise ratio by factors of up to 10 for turbid samples. It also provided for real-time noise monitoring, an important tool for optimal alignment of the pump−probe optics. Noise performance was near shot noise-limited; the rms noise in ΔA was $\sim 10^{-5}$ for 1 s accumulation time.

Steady-State Spectroscopy. The ($P_{700}^+ - P_{700}$) difference spectrum was measured using a UV−vis spectrometer Cary 300 Bio (Varian) that was modified to incorporate an automated 3 V incandescent flashlamp in order to illuminate the sample with light pulses of controlled intensity and duration. The solution of PS I was divided between two 1 cm thick optical cells, which were placed into sample and reference channels of the spectrometer in order to resolve small absorption differences ΔA between sample and reference. The cell in sample channel was subjected to 4 s long light flash leading to oxidation of the special pair into the P_{700}^+ state, while the second cell in the reference channel was kept in the dark at all times. The slow ΔA kinetics associated with the reduction of P_{700}^+ was measured immediately after the light was turned off.

Sample Preparation. The growth, extraction and purification methods of PS I complexes from the *menB* mutant strain of *Synechocystis* sp. PCC 6803 as well as PS I complexes from the wild-type (WT) strain were described earlier.[23] Both *menB* PS I and WT PS I exhibited similar steady-state absorption spectra as shown in Figure 2. For picosecond measurements the solution was diluted with Tris-HCl buffer at pH 8.0 to a final optical density (OD) of 0.93 at 680 nm in a 0.7 mm path length spinning cell. Sodium L-ascorbate (20 mM) and *N*-methylphenazonium methyl sulfate (PMS, 20 μM) were added to the sample to ensure fast reduction of P_{700}^+. The final solution contained 0.06% *n*-dodecyl-β-D-maltoside, a detergent used to minimize aggregation of the PS I complexes.

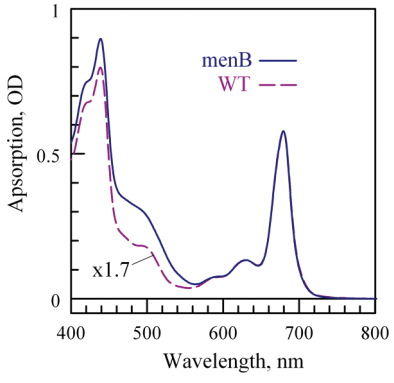

Figure 2. Absorption spectrum of WT PS I and *menB* PS I mutually normalized in the Q_y region.

For steady-state ΔA measurements Tri-HCl at pH 8.0 was added to an absorption of 1.05 OD at maximum (680 nm) in a 1 cm path length cell. The buffer contained small amount of detergent (0.02% β-DM) to avoid aggregation of the protein complexes. Only sodium L-ascorbate at 40 mM was added to the sample (no PMS) to result in a slow (∼25 s) reduction of the P_{700}^+ that could be resolved by the standard UV−vis spectrometer. All experiments were performed at room temperature.

EXPERIMENTAL RESULTS AND DISCUSSION

The ($P_{700}^+A_0^-$ − $P_{700}A_0$) Difference Spectrum. The 10−30 ps dynamics of electron transfer from A_0^- to A_1 in wild-type PS I from *Synechocystis* sp. PCC 6803 (hereafter known as WT PSI)[15,22,28] is comparable to the ∼25 ps overall trapping time of the electronic excitation in antenna pigments by the RC core.[26,29−36] Therefore, the A_0^- state never accumulates in large quantities in WT PS I, as shown in Figure 3a, and the $P_{700}^+A_0^-$ spectrum cannot be resolved clearly. Indeed, the major decay component of the broad band near 685 nm stems from antenna excitation trapping and the formation of $P_{700}^+A_1^-$, and the absorption difference spectrum at times ≥60 ps represents the well-characterized ($P_{700}^+ - P_{700}$) difference spectrum since all electron transfers within the six Chl *a* molecules of the RC core occur at faster rates.[4] In contrast, we found that, under the repetitive flash experiments carried out here, electron transfer from the primary electron acceptor A_0^- in *menB* PS I is significantly slower and occurs in the nanosecond time range.

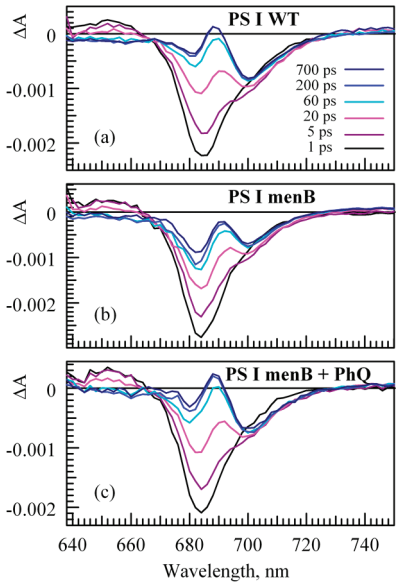

Figure 3. ΔA spectra of WT PS I (a), *menB* PS I (b), and *menB* PS I incubated for ∼48 h with PhQ (PS I/PhQ ratio 1:200) (c) taken at 1, 5, 20, 60, 200, and 700 ps after 635 nm excitation. The signal at long delay times (>100 ps) in PS I WT corresponds to the long-living oxidized state of PS I. The extra ∼684 nm long-living band monitored in PS I *menB* (b), on top of the P_{700}^+ signal, is representative of the A_0^- state. The addition of PhQ to the *menB* PS I sample restores the WT-like amplitude.

The longer lifetime of A_0^- in *menB* PS I in vitro, which is characterized by the ∼684 nm band in Figure 3b, allows us to clearly resolve the $P_{700}^+A_0^-$ absorption spectrum at times ≥60 ps, when the energy transfer to the RC is complete in the PS I core. Figure 3b shows the ΔA spectrum recorded at different time delays after the excitation pulse for *menB* PS I. While the fast processes in this mutant are similar to WT PS I, the

dx.doi.org/10.1021/jp211246a | J. Phys. Chem. B 2012, 116, 3380−3386

absorption difference spectra at ≥60 ps for the *menB* PS I clearly deviate from the known ($P_{700}^+ - P_{700}$) spectrum and are characterized by the presence of an extra band at ~684 nm. Note that the wild-type PS I-like kinetics are completely restored in *menB* PS I complexes after incubation with large quantities of PhQ, the native acceptor in the A_1 sites, as shown in Figures 3c and 4. The similarity of the kinetics for the latter

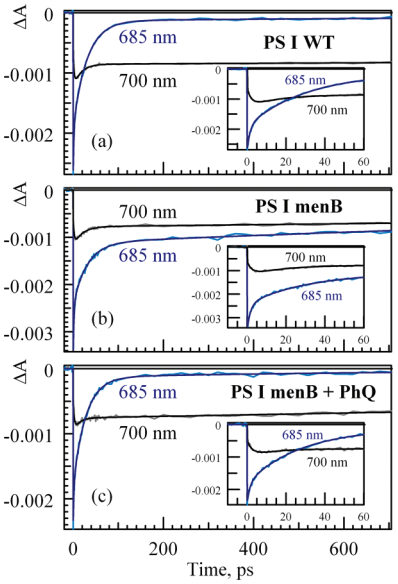

Figure 4. Kinetics of WT PS I (a), *menB* PS I (b), and *menB* PS I incubated for ~48 h with PhQ (1:200) (c) at 700 nm, characteristic of the oxidized special pair (and therefore of the PS I complex activity level), and 685 nm, representative of both the reduced special pair and the oxidized first electron acceptor. The samples were excited at 635 nm.

Table 1. Exponential Fitting Components and Relative Amplitudes of Pump–Probe Kinetics Measured at 685 and 700 nm after Exciting Samples at 660 nm[a]

PS I WT		PS I *menB*		PS I *menB* + PhQ	
685 nm	700 nm	685 nm	700 nm	685 nm	700 nm
1.5 ps (29.8%)	2.2 ps (44.5%), rise	1.8 ps (30.6%)	2.5 ps (44.6%), rise	1.6 ps (25.0%)	2.9 ps (49.5%), rise
31 ps (65.3%)	17 ps (31.1%)	31 ps (37.4%)	19 ps (35.2%)	28 ps (69.5%)	11 ps (26.0%)
1.9 ns (4.9%)	24 ns (68.9%)	2.7 ns (32.0%)	7 ns (64.8%)	0.8 ns (5.4%)	5.6 ns (74.0%)

[a]Note that the nanosecond components are to be taken only as indicative of a long-lived state since they are significantly longer than the measurement time window of 0.7 ns.

sample with WT PS I (Figure 4 and Table 1) indicates that the integrity of the *menB* PS I complexes is not altered by the mutation and validates its use as a representative of WT PS I.

While the Δ*A* band at ~700 nm is roughly identical for both samples, indicating the formation of the P_{700}^+ radical, an extra photobleached band at ~684 nm is formed in *menB* PS I that is absent in WT PS I (Figure 5). The width, position, and intensity of this band are consistent with the formation of an extra Chl a^- radical. We ascribe it to a long-lived A_0^- state that

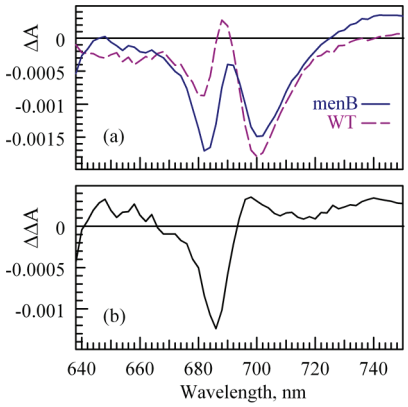

Figure 5. Superposition of the Δ*A* spectra taken 200 ps after excitation for both WT PS I and *menB* PS I (a). The difference (b) between the two spectra indicates the presence of an extra Chl a^- in the *menB* PS I complexes.

is present when the electron pathway from A_0 to the next electron acceptor is either blocked or significantly slowed.

The spectrum in Figure 5b therefore represents the ($A_0^- - A_0$) difference spectrum. However, Figure 5 compares Δ*A* spectra obtained for different samples: the ($P_{700}^+ - P_{700}^-$) difference spectrum was measured for the WT, while the ($P_{700}^+A_0^- - P_{700}^+A_0$) difference spectrum was measured for *menB* PS I. It would be more appropriate if the ($P_{700}^+ - P_{700}^-$) would also be measured for the *menB* PS I sample.

The ($P_{700}^+ - P_{700}$) Difference Spectrum. The ($P_{700}^+ - P_{700}$) difference spectrum was measured using a steady-state absorption spectrometer as described earlier.[22] It is well-known that the charge recombination between the terminal electron acceptor $F_{A/B}^-$ and P_{700}^+ in vitro occurs in ~50 ms.[37] However, a measurable fraction of the electrons are instead scavenged from the terminal electron acceptors[22,38] before recombination can occur between $F_{A/B}^-$ and P_{700}^+. Several seconds of CW illumination thus causes a population buildup of a long-living P_{700}^+ state. The consequent reduction of P_{700}^+ can only occur in the presence of external electron donors such as sodium ascorbate or phenazine methosulfate (PMS). Our experiments show that in the presence of 40 mM ascorbate the reduction of P_{700}^+ in WT PS I occurs with a lifetime of ~25 s which enables the detection of the ($P_{700}^+ - P_{700}$) difference spectrum using a standard steady-state spectrometer operated in kinetic mode. Figure 6b shows the Δ*A* kinetics measured at 700 nm after a 4 s light flash using a standard UV–vis absorption spectrometer. Similar kinetics were measured at multiple wavelengths, globally fitted with a monoexponential decay function, and the respective amplitudes assembled into the ($P_{700}^+ - P_{700}$) difference spectrum shown in Figure 6a. The spectrum from

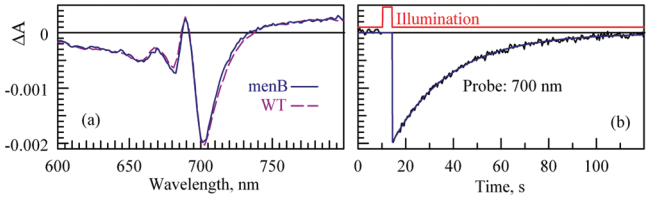

Figure 6. (a) ($P700^+ - P700$) difference spectra of WT PS I, and *menB* PS I are nearly identical. (b) *menB* PS I 700 nm kinetics after 4 s illumination, fitted with ~25 s lifetime. Note that the recovery rate of PS I is proportional to the ascorbate (electron donor) concentration.

dx.doi.org/10.1021/jp211246a | *J. Phys. Chem. B* 2012, 116, 3380–3386

menB PS I is almost identical to WT PS I, a result consistent with the fact that the only difference between the two samples resides in the A_1 quinone binding pockets located relatively far away from the special pair.

The (A_0^- − A_0) Difference Spectrum. The (A_0^- − A_0) difference spectrum was obtained by subtracting the (P_{700}^+ − P_{700}) difference spectrum (Figure 5) from the ($P_{700}^+A_0^-$ − $P_{700}A_0$) difference spectrum (Figure 3). Since the two spectra were measured using different experimental setups, the amplitudes had to be mutually normalized (Figure 7a). The

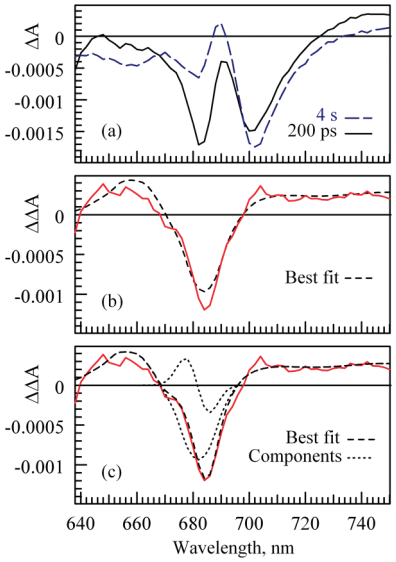

Figure 7. (a) Difference spectra taken 200 ps and 4 s after excitation for *menB* PS I. (b) (200 ps − 4 s) spectrum (solid) and best fit using the shifted in vitro (Chl a^- − Chl *a*) spectrum digitized from[39] (dashed). (c) (200 ps − 4 s) spectrum (solid) and best fit (dashed) using the shifted in vitro (Chl a^- − Chl *a*) spectrum from[39] (dotted) and a 1.7 nm electrochromic blue shift of a 682 nm Chl *a* pigment (dotted).

normalization factor for the (P_{700}^+ − P_{700}) difference spectrum was chosen so that the difference between the spectra would provide the best fit to the typical (Chl a^- − Chl *a*) difference spectrum[39] that is shown in Figure 7b. Since the latter spectrum was measured for Chl *a* in solution, its maximum bleaching had to be red-shifted to match the Δ*A* difference spectrum obtained for A_0^-.

The (A_0^- − A_0) difference spectrum obtained in this way exhibits a maximum at 684 nm (Figure 7b), and is independent of variations in the normalization factor of the ($P_{700}^+A_0^-$ − $P_{700}A_0$) difference spectrum (Figure 7a) within ±20%. Larger variations in this factor lead to difference spectra that are clearly inconsistent with the absorption of a single Chl *a* pigment. A comparison of the A_0 spectrum obtained in the current work with previous data reveals that chemical treatment with sodium dithionite, which is used by a number of groups to reveal the A_0 spectrum, as well as the partial removal of Chl *a* antenna, leads to noticeable red shift of the A_0 band: 693 nm for refs 12 and 13, 690 nm for refs 14 and 20, and 688 nm for ref 15. The model-dependent methods give results close to our findings: 685 nm for ref 21 and 686 nm for refs 15, 16, and 22. Note that in our earlier study[40] we also placed A_0 absorption maximum at 686 nm based on the modeling of the electrochromic absorption shift signal that occurs in response to the electric field from the electron residing on A_1. However, in addition to the A_0 contribution this signal had comparable contributions from three other nearby pigments, which inevitably influenced the precision of the inferred A_0 spectral maximum. In the present study, (A_0^- − A_0) is measured directly and does not have such uncertainty.

Assuming the (P_{700}^+ − P_{700}) extinction coefficient is similar to that measured earlier for PS I complexes extracted from spinach, i.e., 64 mM^{-1} cm^{-1} (at maximum ~700 nm),[41] we can extrapolate that the (A_0^- − A_0) difference spectrum in Figure 7b has an extinction coefficient of ~43 mM^{-1} cm^{-1} at 684 nm, which is in good agreement with previous estimates of 46[18] and 45 mM^{-1} cm^{-1}.[13]

The slight differences between the (A_0^- − A_0) and the (Chl a^- − Chl *a*) spectra represented in Figure 7b can be caused by differences in the environments of A_0 and free Chl *a* in solution. Additionally, the observed differences can be caused by the electrochromic shift experienced by the pigments that are adjacent to A_0^- in a manner similar to the electrochromic shift observed due to the formation of A_1^- in ref 40. This interpretation is plausible because the difference between the A_0^- spectrum and the fit has a clear bipolar profile around 680 nm that is characteristic for an electrochromic shift of an absorption band. To investigate this possibility, we performed simulations of the expected electrochomic shift according to ref 42 using the published structures of PS I.[3,43] The simulations indicate that, independent of the active electron-transfer branch, the main contribution to the difference spectrum of Figure 7b is most likely due to an accessory pigment that is ~8 Å away from A_0 (center to center) and whose absorption is expected to be blue-shifted because of its dipole moment orientation with respect to A_0. The second nearest pigment to A_0 is the connecting pigment A_{40} or B_{39} for branch A and B respectively (~12 Å from respective A_0, Figure 1). However, the angular orientation of its dipole moment change upon excitation ($\Delta\mu$) in respect to the electric field created by nearby A_0^- is ~90° and no significant electrochromic shift is expected. We therefore fitted the (A_0^- − A_0) difference spectrum using both the in vitro (Chl a^- − Chl *a*) difference spectrum from ref 39 and the modeled electrochromic shift spectrum of the accessory pigment (Figure 7c). The electrochromic shift signal was modeled using a simulated Chl spectrum with a shape and oscillator strength similar to the (A_0^- − A_0) band. The best fit was obtained with a 1.7 nm blue shift of the accessory pigment absorption band in the presence of an electron on A_0 provided that the absorption band maximum of the former is at ~682 nm. Figure 8 illustrates the sensitivity of the fit to variations in the spectral position of the accessory pigment absorption band and in the magnitude of its electrochromic shift. In Figure 8a, the position of the accessory Chl band was fixed at λ = 680 nm and at λ = 685 nm, while the other parameters (electrochromic shift, the position and amplitude of A_0) were optimized for best fit, resulting in χ^2 values 1.38 and 1.76 times larger than in the case of the best fit (λ = 682.4 nm), respectively. In Figure 8b, the electrochromic shift of the accessory Chl absorption band was fixed at $\Delta\lambda$ = −0.7 and $\Delta\lambda$ = −2.7, while its position and the position and amplitude of A_0 were optimized, resulting in χ^2 values 1.27 and 1.20 times larger than in the case of the best fit ($\Delta\lambda$ = −1.7), respectively.

Using the suggested parameters from ref 40 for the permanent dipole moment ($\Delta\mu$ = 0.5 D/f) and polarizability ($\Delta\alpha$ = 1.5 $Å^2$ f^{-3}), the 1.7 nm shift of the accessory pigment absorption band implies an effective local dielectric constant ranging from 2 to 3 depending on the RC branch (A or B) for

dx.doi.org/10.1021/jp211246a | *J. Phys. Chem. B* 2012, 116, 3380−3386

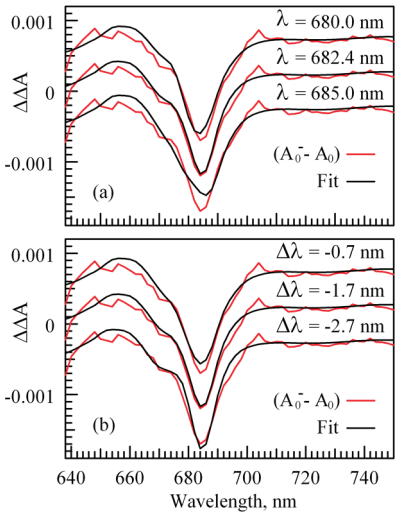

Figure 8. Dependence of the fit (black) of the $(A_0^- - A_0)$ spectrum (red) on variations in the position of the accessory Chl absorption band (a) and on the magnitude of its electrochromic shift (b). Fits are displaced along the vertical axis for clarity. In both planes, the center fit is the best fit obtained when the accessory pigment absorption band is at λ = 682.4 nm. It shifts by $\Delta\lambda = -1.7$ nm in the presence of the electric field created by A_0^-.

which the calculations are made. Note that in ref 40 the estimated local dielectric constant at the position of A_0 for an electron located on A_1 was ~7. A higher dielectric constant at this position is expected due to the presence of significant number of water molecules near the A_1 cofactors that would screen the electric field of A_1^- anion. In contrast, no water molecules were resolved near A_0 and the accessory Chls in the crystal structure of cyanobacterial PS I. An effective dielectric constant of 3 was predicted by calculations[44] for the protein domain between P_{700} and A_0, in agreement with our results. Assuming that the recorded $(A_0^- - A_0)$ signal is a superposition of the A_0^- bleaching and the electrochromic shift of the accessory pigment, this would place the A_0 band maximum at 682 nm and change the extinction coefficient of this band to ~48 mM^{-1} cm^{-1}.

Directionality of Electron Transfer in PS I RC from *Synechocystis* sp. PCC 6803. The data and analysis presented in this work do not provide direct information on the directionality of electron transfer in PS I. However, the Q_y positions of A_0 and the accessory pigments determined in our experiments can be compared to the transition energies of PS I pigments calculated earlier using the semiempirical INDO/S method.[45] According to latter calculations, the A_0 pigments in the A-branch and B-branch of the RC have absorption maxima at 685 and 679 nm, corresponding to the eC-A3 and eC-B3 pigments as denoted in ref 41, respectively, and the neighboring accessory pigments (eC-B2 and eC-A2) absorb at 682 nm in the A-branch and at 668 nm in the B-branch (Figure 1). Our data is more compatible with the pigments in the A-branch, suggesting that electron transfer in the case of cyanobacteria proceeds primarily along this branch. This is in good agreement with earlier other reports.[7−10]

Excitonic Coupling in RC of PS I. The measured $(A_0^- - A_0)$ spectrum is very similar in shape to the (Chl a^- − Chl a) spectrum in solution (Figure 7b), which indicates that excitonic coupling of A_0 with the neighboring pigments are not significant in our experimental conditions. Indeed, excitonic coupling between A_0 and its closest neighbor—an accessory pigment—was estimated to be between 35 and 181 cm^{-1},[45,46] which is lower than thermal energy kT ~ 200 cm^{-1} at room temperature. The excitonic effects (several bands in the ΔA spectrum) have been observed earlier in pump−probe ΔA signals for PS I, but at a much lower temperature of 20 K (kT = 14 cm^{-1}) and only under conditions when (possibly several) excitonic states were excited at ~700 nm.[46]

CONCLUSION

The $(A_0^- - A_0)$ difference spectrum was resolved for the first time without the use of strong reducing agents. Its bleaching band is maximial at 684 nm and it has an oscillator strength of 43 mM^{-1} cm^{-1}. There is also indication that an electrochromic shift of the nearby accessory Chl pigment may contribute ~20% in amplitude to the measured $(A_0^- - A_0)$ signal; in this case the Q_y absorption maxima of both accessory and A_0 Chls are ~682 nm and the oscillator strength of the latter is ~48 mM^{-1} cm^{-1}.

AUTHOR INFORMATION

Corresponding Author

*Phone: (765) 494 3017. Fax: (765) 494-0706. E-mail: sergei@purdue.edu.

Notes

The authors declare no competing financial interest.

ACKNOWLEDGMENTS

The authors gratefully acknowledge the Division of Chemical Sciences, Geosciences, and Biosciences, Office of Basic Energy Sciences of the U.S. Department of Energy, through Grant DE-FG02-09ER16084 for funding studies on optical resolution of A_0 (A.C., N.D., S.S.). This work was also supported in part by a grant from the National Science Foundation (MCB-1021725 to J.H.G.) and by Susquehanna University (T.W.J.).

REFERENCES

(1) Amunts, A.; Nelson, N. *Struct., Cell Press* **2009**, *17*, 637.
(2) Busch, A.; Hippler, M. *Biochim. Biophys. Acta* **2010**, *1807*, 864.
(3) Jordan, P.; Fromme, P.; Witt, H. T.; Klukas, O.; Saenger, W.; Krauss, N. *Nature* **2001**, *411*, 909.
(4) Savikhin, S. Ultrafast Optical Spectroscopy of Photosystem I. In *Photosystem I: the light-driven plastocyanin: ferredoxin oxidoreductase*; Golbeck, J. H., Ed.; Springer: New York, 2006; p 155.
(5) Müller, M. G.; Slavova, C.; Luthrab, R.; Redding, K. E.; Holzwarth, A. R. *PNAS Early Ed.* **2010**.
(6) Holzwarth, A. R.; Müller, M. G.; Niklas, J.; Lubitz, W. *Biophys. J.* **2006**, *90*, 552.
(7) Xu, W.; Chitnis, P. R.; Valieva, A.; van der Est, A.; Brettel, K.; Guergova-Kuras, M.; Pushkar, Y. N.; Zech, S. G.; Stehlik, D.; Shen, G.; Zybailov, B.; Golbeck, J. H. *J. Biol. Chem.* **2003**, *278*, 27876.
(8) Dashdorj, N.; Xu, W.; Cohen, R. O.; Golbeck, J. H.; Savikhin, S. *Biophys. J.* **2005**, *88*, 1238.
(9) Cohen, R. O.; Shen, G.; Golbeck, J. H.; Xu, W.; Chitnis, P. R.; Valieva, A. I.; Van der Est, A.; Pushkar, Y.; Stehlik, D. *Biochemistry* **2004**, *43*, 4741.
(10) Guergova-Kuras, M.; Boudreaux, B.; Joliot, A.; Joliot, P.; Redding, K. *Proc. Natl. Acad. Sci. U.S.A.* **2001**, *98*, 4437.
(11) Soukoulis, V.; Savikhin, S.; Xu, W.; Chitnis, P. R.; Struve, W. S. *Biophys. J.* **1999**, *76*, 2711.
(12) Nuijs, A. M.; Shuvalov, V. A.; van Gorkom, H. J.; Plijter, J. J.; Duysens, L. N. M. *Biochim. Biophys. Acta* **1986**, *850*, 310.
(13) Shuvalov, V. A.; Nuijs, A. M.; van Gorkom, H. J.; Smit, H. W. J.; Duysens, L. N. M. *Biochim. Biophys. Acta* **1986**, *850*, 319.
(14) Mathis, P.; Ikegami, I.; Setif, P. *Photosynth. Res.* **1988**, *16*, 203.

(15) Hastings, G.; Kleinherenbrink, F. A. M.; Lin, S.; McHugh, T. J.; Blankenship, R. E. *Biochemistry* **1994**, 3193.
(16) Kim, D.; Yoshihara, K.; Ikegami, I. *Plant Cell Physiol.* **1989**, *30*, 679.
(17) Itoh, S.; Iwaki, M.; Ikegami, I. *Biochim. Biophys. Acta* **1987**, *893*, 508.
(18) Shuvalov, V. A.; Klevanik, A. V.; Sharkov, A. V.; Kryukov, P. G.; Ke, B.; Bacon, K. E. *FEBS Lett.* **1979**, *107*, 313.
(19) Kumazaki, S.; Iwaki, M.; Ikegami, I.; Kandori, H.; Yoshihara, K.; Itoh, S. *J. Phys. Chem.* **1994**, *98*, 11220.
(20) Wasielewski, M. R.; Fenton, J. M.; Govindjee, R. *Photosynth. Res.* **1986**, *12*, 181.
(21) White, N. T. H.; Beddard, G. S.; Thorne, J. R. G.; Feehan, T. M.; Keyes, T. E.; Heathcote, P. *J. Phys. Chem.* **1996**, *100*, 12086.
(22) Savikhin, S.; Xu, W.; Martinsson, P.; Chitnis, P. R.; Struve, W. S. *Biochemistry* **2001**, *40*, 9282.
(23) Johnson, T. W.; Shen, G.; Zybailov, B.; Kolling, D.; Reategui, R.; Beauparlant, S.; Vassiliev, I. R.; Bryant, D. A.; Jonesi, A. D.; Golbeck, J. H.; Chitnis, P. R. *J. Biol. Chem.* **2000**, *275*, 8523.
(24) Johnson, T. W.; Zybailov, B.; Jones, A. D.; Bittli, R.; Zech, S.; Stehlik, D.; Golbeck, J. H.; Chitnis, P. R. *J. Biol. Chem.* **2001**, *276*, 39512.
(25) Savikhin, S.; Xu, W.; Soukoulis, V.; Chitnis, P. R.; Struve, W. S. *Biophys. J.* **1999**, *76*, 3278−3288.
(26) Savikhin, S.; Xu, W.; Chitnis, P. R.; Struve, W. S. *Biophys. J.* **2000**, *79*, 1573−1586.
(27) Hasson, K. C. Ph.D. Thesis, Harvard University: Cambridge, MA, 1997.
(28) Brettel, K.; Vos, M. H. *FEBS Lett.* **1999**, *447*, 315.
(29) Gobets, B.; van Stokkum, I. H. M.; Rogner, M.; Kruip, J.; Schlodder, E.; Karapetyan, N. V.; Dekker, J. P.; van Grondelle, R. *Biophys. J.* **2001**, *81*, 407.
(30) Gobets, B.; van Grondelle, R. *Biochim. Biophys. Acta* **2001**, *1507*, 80.
(31) Melkozernov, A. N.; Lin, S.; Blankenship, R. E. *Biochemistry* **2000**, *39*, 1489.
(32) Turconi, S.; Kruip, J.; Schweitzer, G.; Rögner, M.; Holzwarth, A. R. *Photosynth. Res.* **1996**, *49*, 263.
(33) Hastings, G.; Reed, L.; Lin, S.; Blankenship, R. *Biophys. J.* **1995**, *69*, 2044.
(34) DiMango, L.; Chan, C.; Jia, Y.; Lang, M. J.; Newman, J. R.; Mets, L.; Fleming, G. R.; Haselkorn, R. *Biophysics* **1995**, *92*, 2715.
(35) Hastings, G.; Kleinherenbrink, F. A. M.; Lin, S.; Blankenship, R. *Biochemistry* **1994**, *33*, 3185.
(36) Hecks, B.; Wulf, K.; Breton, J.; Leibl, W.; Trissl, H.-W. *Biochemistry* **1994**, *33*, 8619.
(37) Hiyama, T.; Ke, B. *Arch. Biochem. Biophys.* **1971**, *147*, 99.
(38) Diaz-Quintana, A.; Leibl, W.; Bottin, H.; Setif, P. *Biochemistry* **1998**, *37*, 3429.
(39) Fujita, I.; D., M. S.; F., J. *J. Am. Chem. Soc.* **1978**, *100*, 6280.
(40) Dashdorj, N.; Xu, W.; Martinsson, P.; Chitnis, P. R.; Savikhin, S. *Biophys. J.* **2004**, *86*, 3121.
(41) Hiyama, T.; Ke, B. *Biochim. Biophys. Acta* **1972**, *267*, 160.
(42) Kakitani, T.; Honig, B.; Crofts, A. R. *Biophys. J.* **1982**, *39*, 57.
(43) Amunts, A.; Toporik, H.; Borovikova, A.; Nelson, N. *J. Biol. Chem.* **2009**, *285*, 3478.
(44) Semenov, A. Y.; Chamorovsky, S. K.; Mamedov, M. D. *Biofizika* **2004**, *49*, 227.
(45) Damjanovic, A.; Vaswani, H. M.; Fromme, P.; Fleming, G. R. *J. Phys. Chem.* **2002**, *106*, 10251.
(46) Gibasiewicz, K.; Ramesh, V. M.; Lin, S.; Redding, K.; Woodbury, N. W.; Webber, A. N. *Biophys. J.* **2003**, *85*, 2547−2559.